European Journal of Chemistry 13 (1) (2022) 117-125

European Journal of Chemistry

ATLANTA PUBLISHING HOUSE

Pyrrolidinecarbodithioate as a planarity chuck in the search for cis-platin analogues of nickel: Spectral, single crystal X-ray structural, BVS, and CSM analysis of some planar nickel(II) mixed ligand complexes

Kuppukkannu Ramalingam [1,*], Murugesan Saravanan [1,2], Gabriele Bocelli [3], Lara Righi [3], Yurii Chumakov [4] and Andrea Cantoni [3]

[1] *Department of Chemistry, Faculty of Science, Annamalai University, Annamalainagar - 608002, India*
[2] *Perkin Elmer Incorporation, Kerala - 682001, India*
[3] *Department of Chemistry, Universita di Parma, Parco Area Delle Scienze-37a, I-43100, Parma, Italy*
[4] *Institute of Applied Physics, Institute of Applied Physics, Academiei Str. 5, Chisinau, Moldova*

* *Corresponding author at: Department of Chemistry, Faculty of Science, Annamalai University, Annamalainagar - 608002, India.*
e-mail: krauchem@yahoo.com *(K. Ramalingam).*

RESEARCH ARTICLE

10.5155/eurjchem.13.1.117-125.2214

Received: 16 November 2021
Received in revised form: 22 January 2022
Accepted: 26 January 2022
Published online: 31 March 2022
Printed: 31 March 2022

KEYWORDS

Planarity chuck
Triphenylphosphine
Pyrrolidinecarbodithioate
Bond valence sum analysis
1,2-Bis(diphenylphosphino)ethane
Continuous shape measure analysis

ABSTRACT

$[Ni(pyrdtc)(PPh_3)(NCS)]$ (1), $[Ni(pyrdtc)(4\text{-}MP)(NCS)]$ (2), $[Ni(pyrdtc)(PPh_3)(CN)]\cdot H_2O$ (3), $[Ni(pyrdtc)(PPh_3)_2]ClO_4$ (4), and $[Ni(pyrdtc)(\widehat{PP})]BPh_4\cdot 2H_2O$ (5) [where pyrdtc: Pyrrolidine carbodithioate/$\widehat{SS}$, PPh_3: Triphenylphosphine, 4-MP: Tri(4-methylphenyl)phosphine, dppe/$\widehat{PP}$: 1,2-Bis(diphenylphosphino)ethane] have been prepared from the parent bis-dithiocarbamate, $[Ni(pyrdtc)]_2$ (6). The prepared compounds were characterized by electronic, IR, ^1H, ^{13}C, and ^{31}P NMR spectra. In the IR spectra of the compounds, thioureide bands are observed at higher wavenumbers for the mixed ligand complexes 1-5 (1528-1540 cm^{-1}) than the parent compound (1490 cm^{-1}). Cyclic voltammetry showed an increasing order of reduction potentials: $5 << 1 \sim 2 < 3 < 4 <<$ $[Ni(pyrdtc)_2]$ indicating an alleviation of electron density on nickel in the mixed complexes compared to the parent compound. Single crystal X-ray structure of the complexes displayed planar geometry around nickel which is in keeping with their diamagnetism. Bond Valence Sums calculated with the corrected R_{ij} indicated the divalent nature of nickel with predominant covalent interactions. Continuous shape measure analysis of the mixed ligand chromophores stipulates a planar square environment around central nickel atom and deviation to tetrahedral or trigonal bipyramidal variants are absolutely negated. In this study, CSM analysis of *cis*-platin, a clinical anti-cancer agent, showed a comparable shape measure as those of the mixed ligand complexes 1-5. Hence, pyrrolidinecarbodithioate acts as a 'chuck' in compounds 1-5 to stabilize the planar square shape of the nickel chromophores and provides a suitable template to synthesize analogues of *cis*-platin.

Cite this: *Eur. J. Chem.* **2022**, *13(1)*, 117-125 **Journal website**: www.eurjchem.com

1. Introduction

Research on metal-dithiocarbamate compounds has been ruling the roost for more than six decades now because of the remarkable structural assortment and applications in diverse fields [1-7]. In particular, the formation of nano metal sulphides from single source precursors has resulted in a surge of publications [8-11]. Group X dithiolates undergo substitution reactions with soft phosphines and hard nitrogenous bases due to their borderline nature. Detailed structural and spectral studies on a variety of planar $Ni\widehat{SS}/C/N/\widehat{PP}$ chromophores have been undertaken from this laboratory as well as by others [12-18]. Transition metal chalcogenides and phosphine complexes find use as semiconducting, optical magnetic, catalytic materials, and as anti-cancer agents [19-23]. In this connection, it is noteworthy that five of the anticancer drugs approved for treating a variety of testicular, ovarian, lung (NSCLC), head and neck, bladder, gastric cancers, and other malignancies are *cis*-platin, carboplatin and oxaliplatin (worldwide), nedaplatin (Japan) and lobaplatin (China) [24-28]. However, the major dose-limiting toxicity of *cis*-platin is its renal toxicity observed in 28 to 36% of patients during chemotherapy [29]. Therefore, the attempts have been made to identify less toxic nickel(II) analogues of *cis*-platin in the past and a salen complex of nickel was screened and was found to be active [30]. *Cis*-platin activity is related to its ability to bind to nitrogen atom of DNA after its *in vivo* transformation to *cis*-$[Pt(NH_3)_2(H_2O)_2]^{2+}$and most importantly, platinum(II) retains its planarity all over because of the relatively large LFSE associated with it compared to nickel and palladium. Relatively, higher electronegativity of Ni^{2+} (1.75) over Pd^{2+} (1.35) and Pt^{2+} (1.44) favors the formation of octahedral aqua complexes than its congeners at a facile rate, which is not generally desirable for its anticancer activity as a contrast to platinum and palladium. Therefore, the use of divalent nickel in the place of platinum necessitates the stabilization of planarity of coordination environment.

https://dx.doi.org/10.5155/eurjchem.13.1.117-125.2214

$$\mathrm{C_4H_8NH + CS_2 \rightarrow C_4H_8NCS_2H}$$

$$\mathrm{2C_4H_8NCS_2H + NiCl_2{\cdot}6H_2O \rightarrow [Ni(pyrdtc)_2] + 6H_2O + 2HCl}$$

$$\mathrm{[Ni(pyrdtc)_2] + 2PPh_3 + 2NH_4NCS + NiCl_2{\cdot}6H_2O \rightarrow 2[Ni(pyrdtc)(PPh_3)(NCS)] + 2NH_4Cl + 6H_2O}$$

Scheme 1

In our efforts to identify planar divalent nickel analogues of *cis*-platin, pyrrolidinecarbodithioate is used as a 'planarity chuck, which holds the work piece' in this study. Here in, we report the synthesis, infrared, electronic, ^{1}H and ^{13}CNMR spectral, voltammetric and single crystal X-ray structural studies on *bis*(pyrrolidinecarbodithioato)nickel(II)-phosphine /cyanide/thiocyanate and dppe complexes with $\mathrm{Ni\overset{\frown}{SS}PN}$, $\mathrm{Ni\overset{\frown}{SS}PC}$, $\mathrm{Ni\overset{\frown}{SS}P_2}$ and $\mathrm{Ni\overset{\frown}{SS}\overset{\frown}{PP}}$ chromophores. The structural information is used in the evaluation of bond valence sums and continuous shape measure. The continuous shape measure data is used to assess the ruggedness of pyrrolidinecarbodithioate as a 'planarity chuck'.

2. Experimental

2.1. Materials and physical measurements

All the reagents and solvents were commercially available high purity materials (Merck) used as supplied without further purification. FT-IR spectra of the complexes were recorded on an Avatar Nicolet FT-IR spectrophotometer (400-4000 cm^{-1}) as KBr pellets. Electronic spectra of the complexes were recorded on a Hitachi U-2001 spectrophotometer in dichloromethane. Cyclic voltammograms (CV) of the complexes were carried out with ECDA-001 electrochemistry system at a scanning rate of 100 mV/s. A three-electrode system with Ag/AgCl as reference, platinum wire as counter and glassy carbon as working electrode was employed. Tetrabutylammonium perchlorate (TBAP) of 0.1 M concentration was used as supporting electrolyte. ^{1}H-, ^{13}C-, and ^{31}P-NMR spectra of the complexes were recorded on an AMX 400 instrument with $\mathrm{CDCl_3}$ as solvent and chemical shifts are reported with reference to TMS and $\mathrm{H_3PO_4}$.

2.2. X-ray crystallography

The intensity data were collected on a Bruker AXS smart single crystal diffractometer with CCD, using graphite monochromated Mo-Kα radiation (λ = 0.71073 Å). Absorption corrections were performed with SADABS [31]. The structures were solved by direct methods with SHELXL NTV 5.1 and refined by SHELXL and OLEX-2 [32,33]. All the non-hydrogen atoms were refined anisotropically and all the hydrogen atoms were fixed geometrically. Molecular plots were drawn with the help of ORTEP [34] and Mercury [35]. Repeated crystallization of compound **5** resulted in crystals with poor X-ray diffracting ability and hence the number of observed reflections were very low which resulted in higher 'R' (Number of reflections collected: 12503; Number of observed reflections (> 2σ): 3984).

2.3. Preparations, elemental, spectral and cyclic voltammetric data

Pyrrolidine (1.70 mL, 20 mmol), carbondisulfide (>1.25 mL 20 mmol) in ethanol (20mL) under ammonical medium (1.0 mL of aqueous ammonia) were mixed under ice cold condition(5°C) to form yellow ammoniumpyrrolidinecarbodithioate. To the ammonium pyrrolidinecarbodithioate, aqueous solution of $\mathrm{NiCl_2{\cdot}6H_2O}$ (0.240 g, 10 mmol) was added with continuous stirring. A green precipitate of $\mathrm{[Ni(pyrdtc)_2]}$ was obtained, which was washed with alcohol and was then dried in air. Yield: 80%, Dec. temp.: 210 °C.

All the mixed ligand complexes were prepared from the parent $\mathrm{[Ni(pyrdtc)_2]}$ with the appropriate phosphine, cyanide, and thiocyanate anions. A mixture of $\mathrm{[Ni(pyrdtc)_2]}$ (0.089 g, 0.25 mmol), triphenylphosphine (0.131 g, 0.5 mmol), $\mathrm{NiCl_2{\cdot}6H_2O}$ (0.059 g, 0.25 mmol), and ammonium thiocyanate (0.038 g, 0.5 mmol) in acetonitrile and methanol (2:1, 50 mL) was refluxed for two hours followed by concentration to ca.25 cm^3 and then the solution was filtered and kept for evaporation. After two days, single crystals of compound suitable for analysis were obtained. The preparative procedures for compounds **2**-**5** were identical to the procedure followed for compound **1.** Reactants for [Ni(pyrdtc)(4-MP)(NCS)] (**2**): $\mathrm{[Ni(pyrdtc)_2]}$ (0.089 g, 0.25 mmol), tri(4-methylphenyl)phosphine (0.153 g, 0.5 mmol), $\mathrm{NiCl_2{\cdot}6H_2O}$ (0.059 g, 0.25 mmol) and ammonium thiocyanate (0.038 g, 0.5 mmol). Reactants for $\mathrm{[Ni(pyrdtc)(PPh_3)(CN)]{\cdot}H_2O}$ (**3**): $\mathrm{[Ni(pyrdtc)_2]}$ (0.089 g, 0.25 mmol), triphenylphosphine (0.131 g, 0.5 mmol), $\mathrm{NiCl_2{\cdot}6H_2O}$ (0.059 g, 0.25 mmol) and potassium cyanide (0.033 g, 0.5 mmol). Reactants for $\mathrm{[Ni(pyrdtc)(PPh_3)_2]\,ClO_4}$ (**4**): $\mathrm{[Ni(pyrdtc)_2]}$ (0.089 g, 0.25 mmol), triphenylphosphine (0.262 g, 1.0 mmol), $\mathrm{NiCl_2{\cdot}6H_2O}$ (0.059 g, 0.25 mmol) and $\mathrm{NH_4ClO_4}$ (0.059 g, 0.5 mmol). Reactants for $\mathrm{[Ni(pyrdtc)(dppe)]BPh_4{\cdot}2H_2O}$ (**5**): $\mathrm{[Ni(pyrdtc)_2]}$ (0.089 g, 0.25 mmol), 1,2-bis(diphenylphosphino)ethane (0.199 g, 0.5 mmol), $\mathrm{NiCl_2{\cdot}6H_2O}$ (0.059 g, 0.25 mmol) and $\mathrm{NaBPh_4}$ (0.086 g, 0.15 mmol). The general reaction sequence is given in Scheme 1.

Pyrrolidinecarbodithioato(isothiocyanato)(triphenylphosphine)nickel(II) (**1**): Color: Purple. Yield: 70%. Dec. temp.: 185 °C. FT-IR (KBr, ν, cm^{-1}): 1533 ($\nu_{\mathrm{C\text{-}N(thioureide)}}$), 2094 ($\mathrm{NC(S)^-}$). ^{1}H NMR (400 MHz, $\mathrm{CDCl_3}$, δ, ppm): 3.48-3.52 (t, 4H, $\mathrm{N}CH_2\mathrm{CH_2}$, ^3J = 6.7 Hz), 1.82-1.95 (m, 4H, $\mathrm{NCH_2}CH_2$), 7.30-7.61 (m, 15H, $\mathrm{PPh_3}$). ^{13}C NMR (100 MHz, $\mathrm{CDCl_3}$, δ, ppm): 198.9 ($\mathrm{NCS_2}$, thioureide), 49.1 ($\mathrm{NCH_2}$), 24.2 ($\mathrm{CH_2}$). ^{31}P NMR (162 MHz, $\mathrm{CDCl_3}$, δ, ppm): 19.9 (P, $\mathrm{PPh_3}$). Anal. calcd. For $\mathrm{C_{24}H_{23}N_2NiPS_3}$: C, 54.83; H; 4.39; N, 5.29. Found: C, 54.87; H, 4.42; N, 5.33%. UV/Vis ($\mathrm{CH_2Cl_2}$, $\lambda_{\max}$, nm, (OD)): 480 (4.45). CV (mV): -1006.

Pyrrolidinecarbodithioato(isothiocyanato) (tri(4-methylphenyl)phosphine)nickel(II) (**2**): Color: Purple. Yield: 73%. Dec. Temp.: 187 °C. FT-IR (KBr, ν, cm^{-1}): 1531 ($\nu_{\mathrm{C\text{-}N(thioureide)}}$), 2099 ($\mathrm{NC(S)^-}$). ^{1}H NMR (400 MHz, $\mathrm{CDCl_3}$, δ, ppm): 3.55-3.60 (t, 4H, $\mathrm{N}CH_2\mathrm{CH_2}$, ^3J = 6.5 Hz), 1.85-1.95 (m, 4H, $\mathrm{NCH_2}CH_2$), 7.30-7.61 (m, 15H, $\mathrm{PPh_3}$). ^{13}C NMR (100 MHz, $\mathrm{CDCl_3}$, δ, ppm): 199.1 ($\mathrm{NCS_2}$, thioureide), 49.2 ($\mathrm{NCH_2}$), 24.4 ($\mathrm{CH_2}$). ^{31}P NMR (162 MHz, $\mathrm{CDCl_3}$, δ, ppm): 15.9 (P, $\mathrm{PPh_3}$). Anal. calcd. For $\mathrm{C_{27}H_{29}N_2NiPS_3}$: C, 57.11; H, 5.10; N, 4.90. Found:C, 57.15; H, 5.15; N, 4.94%. UV/Vis ($\mathrm{CH_2Cl_2}$, $\lambda_{\max}$, nm, (OD)): 480 (4.65). CV (mV): -1010.

Cyanopyrrolidinecarbodithioato(triphenylphosphine) nickel (II) hydrate (**3**): Color: Red. Yield: 68%. Dec. Temp.: 190 °C. FT-IR (KBr, ν, cm^{-1}): 1528 ($\nu_{\mathrm{C\text{-}N(thioureide)}}$), 2112 ($\mathrm{CN^-}$). ^{1}H NMR (400 MHz, $\mathrm{CDCl_3}$, δ, ppm): 3.48-3.57 (t, 4H, $\mathrm{N}CH_2\mathrm{CH_2}$, ^3J = 6.4 Hz), 1.55-1.61 (m, 4H, $\mathrm{NCH_2}CH_2$), 7.31-7.62 (m, 15H, $\mathrm{PPh_3}$). ^{13}C NMR (100 MHz, $\mathrm{CDCl_3}$, δ, ppm): 200.6 ($\mathrm{NCS_2}$, thioureide), 49.0 ($\mathrm{NCH_2}$), 24.3 ($\mathrm{CH_2}$). ^{31}P NMR (162 MHz, $\mathrm{CDCl_3}$, δ, ppm): 29.4 (P, $\mathrm{PPh_3}$). Anal. calcd. for $\mathrm{C_{24}H_{25}N_2NiOPS_2}$: C, 56.35; H, 4.88; N, 5.43. Found: C, 56.38; H, 4.92; N, 5.48%. UV/Vis ($\mathrm{CH_2Cl_2}$, $\lambda_{\max}$, nm, (OD)): 431 (5.15). CV (mV): -1245.

Pyrrolidinecarbodithioatobis(triphenylphosphine) nickel(II) perchlorate (**4**): Color: Red. Yield: 72%. Dec. Temp.: 200 °C. FT-

IR (KBr, ν, cm^{-1}): 1540 ($\nu_{\text{C-N(thioureide)}}$), 1100 ($ClO_4^-$). ^1H NMR (400 MHz, $CDCl_3$, δ, ppm): 3.24-3.35 (t, 4H, $N\mathit{CH_2}CH_2$, ^3J = 6.2 Hz), 1.51-1.61 (m, 4H, $NCH_2\mathit{CH_2}$), 7.30-7.62 (m, 15H, PPh_3). ^{13}C NMR (100 MHz, $CDCl_3$, δ, ppm): 195.4 (NCS_2, thioureide), 49.5 (NCH_2), 24.1 (CH_2). ^{31}P NMR (162 MHz, $CDCl_3$, δ, ppm): 28.7 (P, PPh_3). Anal. calcd. for $C_{41}H_{38}ClNNiO_4P_2S_2$: C, 59.35; H, 4.58, N, 1.65. Found: C, 59.40; H, 4.62; N, 1.69%. UV/Vis (CH_2Cl_2, λ_{max}, nm, (OD)): 480 (4.67). CV (mV): -1440.

Pyrrolidinecarbodithioato-1, 2-bis(diphenylphosphinoethane)nickel(II) tetraphenylborate (**5**): Color: Red. Yield: 71%. Dec. Temp.: 205 °C. FT-IR (KBr, ν, cm^{-1}): 1529 ($\nu_{\text{C-N(thioureide)}}$), 1434 ($BPh_4^-$). ^1H NMR (400 MHz, $CDCl_3$, δ, ppm): 3.43-3.50 (t, 4H, $N\mathit{CH_2}CH_2$, ^3J = 6.1 Hz), 1.52-1.61 (m, 4H, $NCH_2\mathit{CH_2}$), 7.32-7.60 (m, 15H, PPh_3). ^{13}C NMR (100 MHz, $CDCl_3$, δ, ppm): 197.4 (NCS_2, thioureide), 49.7 (NCH_2), 24.2 (CH_2). ^{31}P NMR (162 MHz, $CDCl_3$, δ, ppm): 61.5 (P, PPh_3). Anal. calcd. for $C_{55}H_{56}BNNiO_2P_2S_2$: C, 68.86; H, 5.85; N, 1.44. Found: C, 68.91; H, 5.89; N, 1.47%. UV/Vis (CH_2Cl_2, λ_{max}, nm, (OD)): 440 (4.17). CV (mV): -892/-808.

3. Results and discussion

3.1. Infrared spectra

FT-IR spectra of the planar Ni(II)-dithiocarbamate complexes show signature bands around 1500 cm^{-1} due to the presence of thioureide group. $[Ni(pyrdtc)_2]$ shows the thioureide stretching band at 1510 cm^{-1} and C-S stretching band at 1050 cm^{-1}. All the mixed ligand compounds reported in this study show a significant increase in both thioureide and C-S stretching wavenumbers (1532, 1096 (**1**), 1531, 1096 (**2**), 1528, 1095 (**3**), 1540, 1090 (**4**), 1529, 1100 (**5**) cm^{-1}). The thioureide band has been used as a measure of the contribution of the thioureide form of the dithiocarbamate ligands and indicates the extent of the delocalization of electron density between nitrogen and carbon. Presence of PPh_3 around Ni(II) increased electron delocalization around the metal compared to the parent *bis*-dithiocarbamate. The band observed around 1090 cm^{-1} corresponds to C-S stretching of the dithiocarbamate moiety. The NC(S) stretch appears at 2094 and 2099 cm^{-1} for compounds **1** and **2**, respectively. The cyanide stretching band appears at 2112 cm^{-1} for compound **3**. Characteristic bands due to ClO_4^- and BPh_4^- anions appeared at 1100 and 1434 cm^{-1} respectively. The C-H stretching of the pyrrolidine ring in all the compounds remain unaffected and is observed ~2920 cm^{-1}.

3.2. Electronic spectra

Electronic spectra of the compounds were recorded in CH_2Cl_2. Electronic spectrum of ammonium pyrrolidinedithiocarbamate showed a $\pi \rightarrow \pi^*$ transition prominently at 350 nm. The $\pi \rightarrow \pi^*$ transition was identified at 380 nm while the $n \rightarrow \pi^*$ transition was observed at 320 nm in the parent $[Ni(pyrdtc)_2]$. Ligand to metal charge transfer transition was observed at 390 nm and the *d-d* transition was observed at 430 nm with relatively low intensity. In this study, *d-d* transitions of the various planar nickel-dithiocarbamate compounds are observed in the range between 430 and 480 nm, due to d_{yz}-d_{xy} transitions [12]. Absorption bands observed around 480 nm in compounds **1**, **2** and **4** are attributed to *d-d* transitions. The cyanide ion and chelating dppe force a relatively larger LFSE and hence the corresponding absorptions were observed at 430 and 440 nm in compounds **3** and **5** respectively.

3.3. Cyclic voltammetry

In all complexes, Ni(II) is reduced to Ni(I) and mixed ligand complexes showed lower reduction potentials than the parent, $[Ni(pyrdtc)_2]$ (-1789 mV). Complex **5** showed relatively a lower reduction potential (-892/-808 mV) than the other four complexes due to the coordination of chelating π-acceptor dppe and underwent a quasi-reversible one-electron reduction while the other complexes underwent irreversible reductions. The quasi-reversible reduction observed in the dppe complex indicates the effective π-acidic cushioning provided by the ligand. As a contrast, the parent $[Ni(pyrdtc)_2]$ complex undergoes an irreversible one-electron reduction at -1789 mV, a large negative potential indicating the reluctance of the metal to add electron density to the already electron rich center [17]. Between the two limiting values of the reduction potentials, complex **3** undergoes reduction at -1245 mV due to the presence of both cyanide ion and PPh_3. Complexes **1** and **2** showed comparable reduction potentials. Following is the increasing order of reduction potentials for the complexes: **5** <<**1** ~ **2** <**3** <**4** << $[Ni(pyrdtc)_2]$.

3.4. NMR spectra

Pyrrolidine shows two ^1H NMR signals at δ 2.75 and 1.59 ppm for $N\mathit{CH_2}CH_2$ and $NCH_2\mathit{CH_2}$ protons, respectively. Similarly, for the ammonium pyrrolidinecarbodithioate the two signals were reported at δ 3.65 (N-CH_2) and 1.84 (C-CH_2) ppm [36]. On complex formation, the protons adjacent to nitrogen ($N\mathit{CH_2}CH_2$) atom undergo strong deshielding whereas the protons away from N-atom ($NCH_2\mathit{CH_2}$) undergo weak deshielding. In complex **1**, $N\mathit{CH_2}CH_2$ protons undergo strong deshielding to give the signal at δ 3.48-3.52 ppm and $NCH_2\mathit{CH_2}$ protons undergo weak deshielding at δ 1.82-1.95 ppm. A similar trend of chemical shifts is observed for compounds **2** to **5** indicating the fact that the protons away from nitrogen are less deshielded compared to those which are adjacent to the nitrogen.

The chemical shifts of the carbon atom of the $>NCS_2$ moiety are correlated to the bonding in the $>NCS_2$ fragment from the ^{13}C NMR spectra of complexes. The thioureide stretching bands are usually observed around 1500 cm^{-1} for *N*,*N*-dialkyldithio carbamates. Complex **1** shows the thioureide band at 1533 cm^{-1} and hence a low ^{13}C chemical shift was observed at δ 198.9 ppm. The cyanide and the isothiocyanate carbon signals are observed merged with the phenyl ring carbons in the δ range 130 and 145 ppm. The $N^{13}CS_2$ signal of compound **4** appears highly deshielded than the other due to the mitigation of electron density on nickel by the presence of two phosphines.

Free triphenylphosphine ^{31}P signal appears at δ equivalent to -5 ppm A coordinated phosphine has a signal at δ 20 ppm, a free chelating dppe has a signal at δ 30 ppm, and a coordinated chelating dppe has a signal at δ 60 ppm [7-9]. ^{31}P signals are observed at δ 29.4, 28.7, 19.9, and 15.9 ppm for NiS_2PC (**3**), NiS_2P_2(**4**), NiS_2PN (**1**), and $NiS_2P(4\text{-}Me)_3N$ (**2**) chromophores, respectively, in the given order. A very high deshielding observed in the case of NiS_2PC (**3**) chromophore indicates a relatively strong coordination of phosphine to nickel compared to others. However, the shift observed in NiS_2P_2(**4**) chromophore is comparable to that observed in compound (**3**). The chemical shifts for the NiS_2PN chromophores show a highly significant deshielding to the extent of δ ~25 ppm compared to the free ligand. $[Ni(pyrdtc)(dppe)]$ BPh_4 (**5**) shows a chemical shift of δ 61.5 ppm, which indicates a significant chelating by dppe.

3.5. Single crystal X-ray structure analysis

Crystal data, data collection, and refinement parameters of the complexes are shown in Table 1. Thermal ellipsoid plots of the complexes are shown in Figures 1-4. Selected bond distances and angles are given in Table 2. In general, nickel atom is approximately in a square planar environment in keeping with the observed diamagnetism of the complexes. Perfect square planar geometry is not observed in the complexes because of small bite angle associated with the pyrrolidinecarbodithioate anion.

Table 1. Crystal data, data collection, and refinement parameters for compounds **1**-**4**.

Compound	**1**	**2**	**3**	**4**
Empirical formula	$C_{24}H_{23}N_2NiPS_3$	$C_{27}H_{29}N_2$ Ni PS_3	$C_{24}H_{25}N_2$ Ni OPS_2	$C_{41}H_{38}ClNNiO_4P_2S_2$
Formula weight	525.33	567.38	511.26	828.92
Temperature (K)	293(2)	293(2)	293(2)	293
Crystal system	Triclinic	Monoclinic	Triclinic	Orthorhombic
Space group	*P*-1	$P2_111$	*P*-1	*Pbca*
a, (Å)	7.791(2)	10.167(2)	9.6420(19)	16.442(2)
b, (Å)	11.763(2)	9.906(2)	10.353(2)	21.627(2)
c, (Å)	14.283(2)	28.077(2)	13.925(3)	21.591(2)
α (°)	96.86(2)	90	85.93(3)	90.00
β (°)	97.70(3)	97.88(3)	89.14(3)	90.00
γ (°)	105.47(2)	90	62.63(3)	90.00
Volume (Å^3)	1233.6(4)	2801.1(8)	1231.1(5)	7677.6(14)
Z	2	4	2	8
ρ_{calc}(g/cm^3)	1.414	1.345	1.379	1.434
μ (mm^{-1})	1.120	0.992	1.041	0.810
F(000)	544.0	1184.0	532.0	3440.0
Crystal size (mm^3)	0.34 × 0.19 × 0.11	0.23× 0.19 × 0.16	0.24 × 0.21× 0.19	0.29 × 0.19 × 0.15
Radiation	MoKα (λ = 0.71073)	MoKα (λ = 0.71073)	MoKα (λ = 0.71073)	MoKα (λ = 0.71073)
2Θ range for data collection (°)	3.64 to 56.476	2.928 to 62.13	2.932 to 60.84	3.64 to 56.90
Index ranges	$-10 \le h \le 10$	$-13 \le h \le 13$	$-13 \le h \le 13$	$-18 \le h \le 21$
	$-15 \le k \le 14$	$-13 \le k \le 13$	$-14 \le k \le 14$	$-21 \le k \le 27$
	$-18 \le l \le 17$	$-35 \le l \le 35$	$-19 \le l \le 19$	$-25 \le l \le 27$
Reflections collected	13527	31234	17505	45499
Independent reflections	5431 [R_{int} = 0.0200, R_{sigma} = 0.0218]	12535 [R_{int} = 0.0497, R_{sigma} = 0.0522]	6676 [R_{int} = 0.0266, R_{sigma} = 0.0353]	8975 [R_{int} = 0.1043, R_{sigma} = 0.2598]
Data/restraints/parameters	5431/0/270	12535/1/613	6676/0/288	8975/0/622
Goodness-of-fit on F^2	1.001	1.004	1.000	0.997
Final R indexes [I≥2σ (I)]	R_1 = 0.0347, wR_2 = 0.0943	R_1 = 0.0426, wR_2 = 0.0968	R_1 = 0.0356, wR_2 = 0.0875	R_1 = 0.0471, wR_2 = 0.0831
Final R indexes [all data]	R_1 = 0.0440, wR_2 = 0.1001	R_1 = 0.0639, wR_2 = 0.1044	R_1 = 0.0641, wR_2 = 0.0960	R_1 = 0.1992, wR_2 = 0.1124
Largest diff. peak/hole (e.Å^{-3})	0.67/-0.45	0.56/-0.54	0.45/-0.31	0.63/-0.39
Flack parameter	-	0.008(7)	-	-

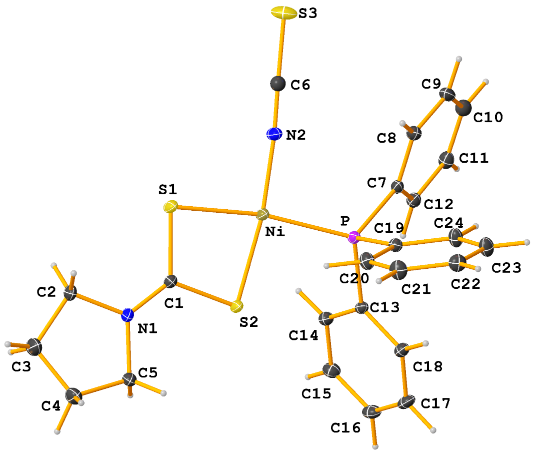

Figure 1. ORTEP diagram of [Ni(pyrdtc)(PPh$_3$)(NCS)] (**1**).

Angular disposition of the planar chromophores is depicted in Figure 5. In complex **1**, the two Ni-S distances are unequal due to the difference in the *trans* influencing property of the NCS$^-$ and PPh$_3$ groups. The PPh$_3$ has higher *trans* influencing ability than the NCS$^-$ group. Hence the Ni-S(1) bond which is *trans* to PPh$_3$ is longer than Ni-S(2) bond which is *trans* to NCS group [Ni-S(1): 2.2365(11) Å, Ni-S(2): 2.1889(7) Å]. The S-Ni-S angle is 78.45(2)°, which is significantly smaller than that observed in the parent dithiocarbamate (79.33(5)°) [37]. Delocalization of π-electron density over S_2CN moiety is evident from the shortening of C-S and C-N bonds and the NCS$^-$ group is slightly bent towards dithiocarbamate group. The thioureide bond distance in compound **1** was found to be 1.303(3) Å. In complex **2** also, the two Ni-S distances are unequal due to the difference in the *trans* influences exerted by the tri(4-methylphenyl)phosphine(4-MP) compared to NCS$^-$. The 4-MP group exerts higher *trans* influence than NCS$^-$ group and hence the two Ni-S distances differ significantly [Ni-S(1): 2.2515(16), Ni-S(2): 2.1756(17) Å] as observed in compound **1**. The observed thioureide distance 1.298(8) Å is comparable to that observed in compound **1**. There is an increase in Ni-P distance due to the steric effect of the 4-methyl substituent. TheN-C-S angles were found to be comparable (177.9(8)°in compound **2** and 178.1(7)° in compound **1**) and are slightly non-linear. However, steric influence of 4-methyl group in compound **2** manifests itself in a highly significant manner in a reduced Ni-N-C(S) angle equivalent to 162.4(6)° compared to 175.08(19)° observed in compound **1**. The Ni-S distances in compound **2** are unequal as observed in compound **1** and the heterolepticity is magnified because of the *trans* influence of the 4-MP. A short thioureide distance (1.298(8) Å) was observed and is in line with the IR spectral observations. In compound **3**, Ni-S distances are asymmetrical [Ni-S(1): 2.2102(7); Ni-S(2): 2.2186(12) Å] and as the cyanide ion which occupies the highest position in spectrochemical series, influences a strong *trans* effect. The Ni-C(N) distance was found to be 1.857(2)Å. The P-Ni-S angle was 175.95(2)°, which indicates near linearity. The P-Ni-C angle was found to be 91.90(7)°. The thioureide distance was observed to be, 1.298(3) Å.

Table 2. Selected bond distances (Å) and angles (°).

Compound	Ni-S(1), Ni-S(2)	Ni-P	Ni-N/Ni-C/Ni-P	C-N	S(1)-Ni-S(2)	P-Ni-P/C/N
1	2.2365(11), 2.1889(7)	2.2087(10)	1.862(2)	1.303(3)	78.45(3)	95.03(7)
2$^{\#}$	2.2515(16), 2.1756(17)	2.2459(15)	1.820(5)	1.259(7)	77.46(6)	90.61(16)
3	2.2186(12), 2.2102(7)	2.1956(11)	1.857(2)	1.298(3)	79.01(3)	91.90(7)
4	2.2250(15), 2.2002(15)	2.2076(15)	2.2268(14)	1.302(6)	78.38(5)	99.66(5)
5	2.228(3), 2.223(3)	2.171(3)	2.178(3)	1.314(12)	79.57(12)	86.55(1)
[Ni(pyrdtc)$_2$] *	2.214(1), 2.198(1)	-	-	1.311(4)	79.33(5)	-

* Reference [37].

$^{\#}$ Bond parameters of one of the two asymmetric units (unprimed) are listed.

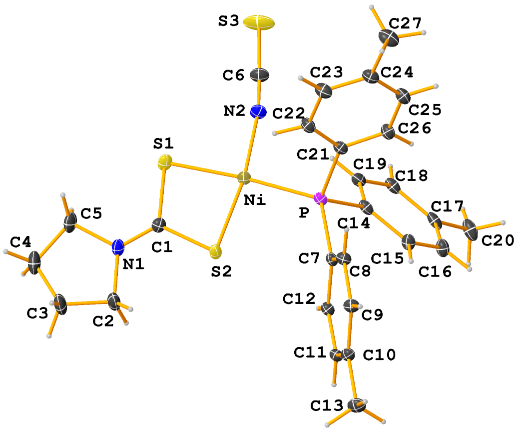

Figure 2. ORTEP diagram of [Ni(pyrdtc)(4-MP)(NCS)] (**2**).

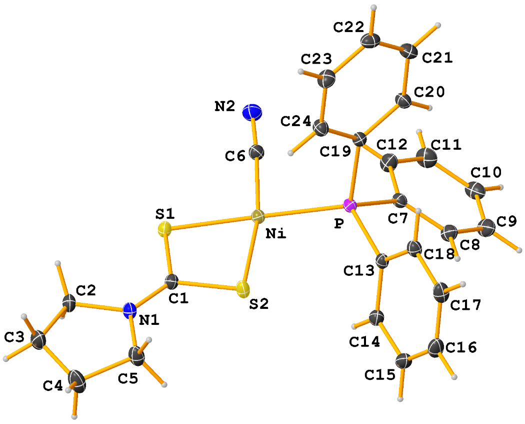

Figure 3. ORTEP diagram of [Ni(pyrdtc)(PPh$_3$)(CN)]·H$_2$O (**3**). Water molecule are not included.

In complex **4**, the Ni-S and Ni-P distances *trans* to each other show a balancing trend with longer Ni-S bond *trans* to short Ni-P bond distance in the molecule and vice-versa. The thioureide distance was found to be 1.302(6) Å. The S-Ni-S angle was found to be 78.38(5)° and the P-Ni-P angle was found to be 99.66(5)°. The perchlorate anion was found to be distorted from tetrahedral geometry. In complex **5**, two water molecules co-crystallized with the molecule and the crystals obtained were of poor crystallinity. However, the Ni-S, Ni-P, and C-N distances from the structure solution are considered for the sake of comparison with the other four compounds. The Ni-S bond distances are almost similar [Ni-S: 2.228(3)-2.223(3) Å] and the S-Ni-S bite angle of the dithiocarbamate was found to be 79.57(12)°. Short Ni-P bond distances observed in the dppe compared to those of its PPh$_3$ analogue is due to the chelating nature of the dppe ligand. The thioureide bond distance is 1.314(12) Å. The two Ni-S distances are longer than the distances observed in other similar dithiocarbamates. The two Ni-P distances [2.171(3) and 2.178(3) Å] are relatively very short and are almost equal considering the respective esd's. The P-Ni-P angle is lower than that observed in complex **4** because of the chelating nature of dppe. From Tables 2 and 3, maximum deviation of nickel atom from the planar square chromophores is observed in compound **1**. Ni-S bond distances in the complexes **1**-**4** are affected to a larger extent by *trans* influence and the steric effect of the substituted phosphines in the coordination environment. It is noteworthy that the S-Ni-S angles of all are close to that observed in the parent *bis*-dithiocarbamate (79.33(5)° [37]).

Compounds **1**-**4** contain monodentate phosphines, thiocyanate or cyanide besides the pyrrolidinecarbodithioate anion. Structurally, a clear heterolepticity in bonding is observed in M-S distances (Mean: short M-S distance: 2.1937(11); long distance: 2.2329(13) Å). Mean Ni-P distance in the reported compounds is 2.2144(13) Å. Interestingly, the mean S-Ni-S angle observed in compounds **1**-**6** is 78.70(7)°, which is significantly less than the ideal right angle. *Trans*-[NiCl$_2$(PPh$_3$)$_2$]·2CH$_2$Cl$_2$ [38] shows an Ni-P distance of 2.2439(5) Å and its tetrahedral analogue [NiCl$_2$(PPh$_3$)$_2$] [39] shows a relatively longer Ni-P distance of 2.3180(2) Å.

Table 3. Bond valence sum of nickel atom and its deviation from the planes.

Compound	**V_{ij}***	**Maximum deviation (Å) of atoms from $\widehat{SS}PN$ / $\widehat{SS}PC$ / $\widehat{SS}PP$/ $\widehat{SS}\widehat{PP}$/ $\widehat{SS}\widehat{SS}$ planes**	**Maximum deviation (Å) of nickel from $\widehat{SS}PN$ / $\widehat{SS}PC$ / $\widehat{SS}PP$/ $\widehat{SS}\widehat{PP}$/ $\widehat{SS}\widehat{SS}$ planes**
[Ni(pyrdtc)(PPh$_3$)(NCS)] (**1**)	2.040	0.0751	0.0682
[Ni(pyrdtc)(4-MP)(NCS)] (**2**)	1.983	0.0354	0.0120
[Ni(pyrdtc)(PPh$_3$)(CN)]·H$_2$O (**3**)	2.042	0.0690	0.0661
[Ni(pyrdtc)(PPh$_3$)$_2$]·ClO$_4$ (**4**)	1.901	0.0751	0.0279
[Ni(pyrdtc)(dppe)]·BPh$_4$(**5**)	2.002	0.1034	0.0738
[Ni(pyrdtc)$_2$]‡ (**6**)	2.178	0.0001	0.0001

*****R_{ij} for Ni-S and Ni-N are from references [44-46]. R_{ij} for Ni-C (1.604 Å) and Ni-P (1.884 Å) are reported from a fit of experimental bond distances for twenty complexes with divalent nickel as the central metal.

‡ Bond parameters are from reference [37].

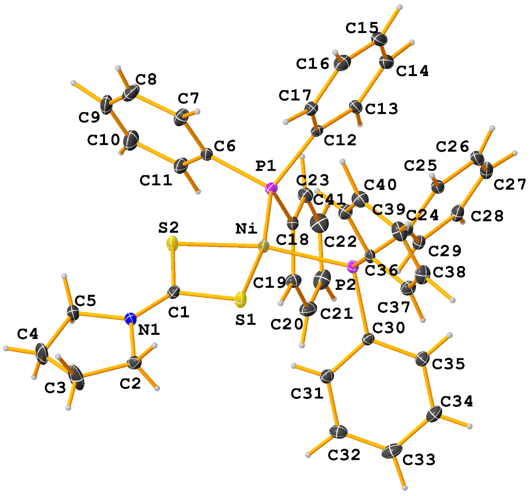

Figure 4. ORTEP diagram of [Ni(pyrdtc)(PPh$_3$)$_2$]ClO$_4$ (**4**). The perchlorate anion is not included.

Ni-Cl distances in the tetrahedral compounds are longer than that observed in the planar form (Tetrahedral: 2.2075(4) Å; Planar square: 2.1672(5) Å). P-Ni-Cl angle in the planar square *trans*-[NiCl$_2$(PPh$_3$)$_2$]·2CH$_2$Cl$_2$ is 93.03(2)°. Its noteworthy, that the Ni-P distances recorded in the present study are longer than the distance reported for *trans*-[NiCl$_2$(PPh$_3$)$_2$]·2CH$_2$Cl$_2$. Comparison of Ni-S bond distances of *trans*-[Ni(SC$_6$H$_5$)$_2$(PMe$_3$)$_2$] (**9**), *trans*-[Ni(SC$_6$H$_4$(o-Me))$_2$(PMe$_3$)$_2$] (**10**) and [Ni(SCOC$_6$H$_5$)$_2$(PPh$_3$)$_2$] (**11**) with the distances observed in compounds **1**-**6** show that they are between the heteroleptic bond distances [Ni-S: 2.2138(5) Å (**9**), 2.2116(7) Å (**10**), 2.231(5) Å (**11**)] [40,41]. But the Ni-P distances are comparable to the distances reported in the present study [Ni-P: 2.2199(7) Å (**9**), 2.2141(8) Å (**10**), 2.156(5) Å (**11**)]. The corresponding S-Ni-P and S-Ni-S bond angles in compounds **9**-**11** clearly indicate that the planar square geometry in compounds **1**-**6** is skewed because of pyrrolidinecarbodithioate anion [S-Ni-P: 93.23(2)° (**9**), 93.49(3)° (**10**), S-Ni-S: 95.0(3) ° (**11**)]. Bond parameters of *cis*-platin (**12**) reported in the literature [Pt-Cl: 2.33(1) Å, Pt-N: 2.01(4) Å, Cl-Pt-N: 90.9(4)°] show that bond angles are close to 90° [42]. However, mean P-Ni-P/C/N angles for compounds **1**-**5** is 92.35(7)° and the variation in the angle depends on the bulkiness of the substituent. The compounds investigated in the present study contain nickel as the central atom which is of lower renal toxicity than platinum. The chelating nature of pyrrolidinecarbodithioate anion adds extra stability to the planar square geometry and nickel(II) shows reluctance to add axial ligands similar to divalent platinum.

3.6. Bond valence sum analysis

The bond valence sum (BVS) model can be used to determine the compatibility between a given coordination model and a particular oxidation state and conversely, the method is used to check correctness of the determined structure. Application of BVS model [43], to divalent nickel coordination complexes always resulted in a higher valence and for many of the dithiocarbamato complexes of divalent nickel, the bond valence sums exceeded 2.8. The increased V_i obtained for Ni^{2+} is due to the use of R_{ij} values obtained from the crystallographic bond distances of homoleptic extended solids, which have predominantly ionic character and in the present study, R_{ij} distances have been redetermined for some model complexes of transition metals with partial covalence [44,45]. The BVS computed for the complexes with the revised R_{ij} [46] are shown in Table 3 and the formal oxidation state for the complexes **1**-**5** are ~2.0 confirming the correctness of the determined crystal structures and the formal oxidation state of the central nickel atom.

3.7. Continuous shape measure analysis of the chromophores

Continuous Shape Measure (CSM) details the extent of distortion of a polyhedron from the ideal symmetry or from reference symmetry [47-49]. Descriptions of geometries such as 'slightly distorted' or 'severely distorted' with reference to a polyhedron is highly qualitative in nature. Degree of distortion of a particular molecular structure from an ideal polyhedron can be assessed by symmetry measures. Table 4 depicts the continuous shape measures of the chromophores evaluated from the structural parameters of the compounds **1**-**6** along with five more complexes which contain similar chromophores **7**-**11** from the published crystal structures for comparison (Figure 5). The CSM values vary from 0 to 100, higher the value, larger is the deviation of a structure from the assigned shape. All the chromophores of compounds **1**-**6** showed CSM ≤ 0.7196 (planar square) confirming their planar square geometry. As a contrast, the assessed values for tetrahedral configuration of the chromophores are relatively large (CSM = 30.5372 - 33.7831), confirming the planar square geometry of the chromophores.

Table 4. Continuous shape measure parameters for the chromophores.

Compound	**Planar Square**	**Tetrahedral**	**Tbp‡ (Uebd)**	**Tbp‡ (Ebd)**
[Ni(pyrdtc)(PPh_3)(NCS)] (**1**)	0.6680	30.5372	24.4955	28.7562
[Ni(pyrdtc)(4-MP)(NCS)] (**2**)	0.5831	32.1472	23.8335	29.7520
[Ni(pyrdtc)(PPh_3)(CN)]·H_2O (**3**)	0.7196	32.8854	23.3066	28.8087
[Ni(pyrdtc)(PPh_3)$_2$]·ClO_4 (**4**)	0.6414	30.5100	24.6447	29.0546
[Ni(pyrdtc)(dppe)]·BPh_4 (**5**)	0.6631	29.4175	23.5953	27.9039
[Ni(pyrdtc)$_2$] (**6**)	0.6759	33.7831	25.9948	30.7708
Planar *trans*-[$NiCl_2(PPh_3)_2$]·$2CH_2Cl_2$^{a}(**7**)	0.1003	33.4002	25.1710	30.2536
Tetrahedral [$NiCl_2(PPh_3)_2$]^b (**8**)	25.4633	0.8986	26.6717	25.4612
Trans-[$Ni(SC_6H_5)_2(PMe_3)_2$]^c (**9**)	0.0800	33.3867	25.7202	30.3933
Trans-[$Ni(SC_6H_4$(o-Me))$_2(PMe_3)_2$]^c (**10**)	0.0930	33.3953	25.7641	30.4152
[Ni(SCO $C_6H_5)_2(PPh_3)_2$]^d (**11**)	0.3850	29.0065	23.9688	28.3971
Cis-[$Pt(NH_3)_2Cl_2$]^e (**12**)	0.5428	33.1362	25.4844	30.3570

‡ Tbp: Triangular bi-pyramid - Total number of atoms: 5 (no central atom) - Uebd: Unequal bond distances; Ebd: Equal bond distances.

[a] Planar square (with central atom) - 5 atoms [38].

[b] Tetrahedron (with central atom) - 5 atoms [39].

[c] Reference [40].

[d] Reference [41].

[e] Reference [42].

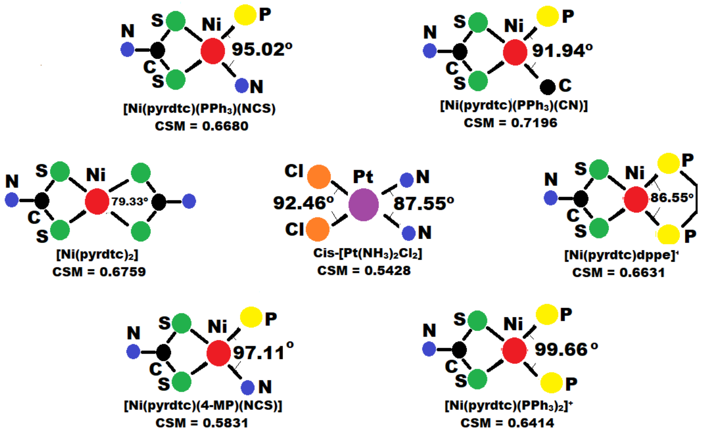

Figure 5. Comparison of CSM and angular dispositions.

A comparison with planar square *trans*-[$NiCl_2$ $(PPh_3)_2$]·$2CH_2Cl_2$ (**7**) and its tetrahedral analogue exemplifies the utility of CSM [45,46]. For compound **7**, CSM (planar square) = 0.1003, CSM (Tetrahedral) = 33.4002, on the contrary, for its tetrahedral analogue (**8**), CSM (planar square) = 25.4633, CSM (Tetrahedral) = 0.8986. CSMs associated with complexes **9**-**11** clearly demonstrate the planar square structures associated with them. Compounds **9** and **10** stabilize as *trans* isomers for steric reasons and are vulnerable to aquation leading to octahedral geometry and lose the mandatory planar geometry. Interestingly, compound **11**, stabilizes in *cis* form but yet again is amenable to aquation. The susceptibility of compounds **9**-**11** to aquation is because of the low LFSE associated with monodentate thiolato donors whereas the "chuck", pyrrolididine carbodithioate anion stabilizes the planar shape. Single crystal X-ray structure of *cis*-platin showed a planar square structure around platinum(II) (**12**) [42]. CSM for planar square shape of the complex **12** is evaluated to be 0.5428 and for tetrahedral geometry it was found to be 33.1362. The CSM values are of the same order as observed for the complexes **1**-**5**. Two other possible shapes *viz.*, trigonal bipyramidal (Uebd) (containing five atoms, no central atom and unequal bond distances) and trigonal bipyramidal (Ebd) (containing five atoms, no central atom and equal bond distances) have been evaluated for all the compounds **1**-**12** and are listed in Table 4. The CSM values for the trigonal bipyramidal variants lie between 23.3066 and 30.7708, clearly ruling out the possibility of the compounds assuming tbp geometry. The CSM analysis of compounds **1**-**12** reveals that compounds **1**-**5** are stabilized in planar square geometry, which is ideal for anti-cancer activity, and have shape measure values comparable to *cis*-platin.

4. Conclusions

Thioureide stretching bands observed for the compounds **1**-**5** are in the range between 1528 and1540 cm^{-1} and are larger than that observed for the parent *bis*-dithiocarbamate *viz.*, 1490 cm^{-1}. The observed increase in ν_{C-N} is because of the π-acidic character of the phosphines enabling a higher delocalization of electron density. ^1H NMR of the complexes show a larger deshielding of the protons adjacent to nitrogen atom compared to the ones away from it. ^{13}C NMR chemical shifts of the thioureide carbon atoms appear in the range δ 195.4-200.6 ppm and correlate well with relatively higher IR stretching bands. ^{31}P NMR chemical shifts of the mixed ligand complexes showed large deshielding with reference to free phosphines signifying strong complexation. In cyclic voltammetric analysis, reduction potentials of the mixed ligand complexes are much lower than their parent dithiocarbamate because of the π-acidic phosphines. In the case of mixed divalent dithiocarbamate complexes investigated in the present study, Ni-S, Ni-P, Ni-N, and Ni-C bond distances and N-Ni-P, N-Ni-P(4-MP), (N)C-Ni-P, and P-Ni-P bond angles varied according to the steric and electronic effects of triphenylphosphine/tri(4-methylphenyl) phosphine/CN^-/dppe. In particular, the Ni-S distances vary in accordance with the variation of *trans* influences of phosphine, cyanide or isothiocyanate leading to heterobidentate binding of the dithiocarbamate. Heterolepticity in Ni-S bond distances is the largest for [Ni (pyrdtc)(4-MP)(NCS)] (**2**) owing to the steric influence of 4-MP. The dppe complex shows the least P-Ni-P angle due its chelating nature. All compounds showed comparable thioureide distances to the parent [Ni(pyrdtc)$_2$]. Bond valence sums revealed that the nickel is divalent and the bonding interactions are primarily covalent. Continuous shape measure analysis of the mixed ligand chromophores clearly specifies a planar square environment around central nickel atom and deviation to tetrahedral or trigonal bipyramidal variants without central atoms is completely negated. In this study, clinically validated cis-platin was subjected to CSM analysis and was found to have a CSM comparable to mixed ligand complexes **1**-**5**. As a distinction, unlike monodentate thiolates, pyrrolidinecarbodithioate acts as a "planarity chuck, which holds the work piece" to stabilize the planar square shape of the nickel chromophores and provides the setting for the steps to mimic *cis*-platin coordination environment. Therefore, pyrrolidinecarbodithioate as a "molecular chuck" in compounds **1**-**5** to stabilize the planar geometry of the nickel chromophores and afford a suitable template for the synthesis of less toxic divalent nickel analogues of *cis*-platin.

Supporting information

CCDC-182725 (**1**), 218293 (**2**), 209868 (**3**), and 182726 (**4**) contain the supplementary crystallographic data for this paper. These data can be obtained free of charge via www.ccdc.cam.ac.uk/data_request/cif, or by e-mailing data_request@ccdc.cam.ac.uk, or by contacting The Cambridge Crystallographic Data Centre, 12 Union Road, Cambridge CB2 1EZ, UK; fax: +44(0)1223-336033.

Disclosure statement

Conflict of interests: The authors declare that they have no conflict of interest.
Ethical approval: All ethical guidelines have been adhered.
Sample availability: Samples of the compounds are available from the author.

CRediT authorship contribution statement

Conceptualization: Kuppukkannu Ramalingam; Methodology: Kuppukkannu Ramalingam; Software: Kuppukkannu Ramalingam; Validation: Kuppukkannu Ramalingam; Formal Analysis: Murugesan Saravanan; Investigation: Kuppukkannu Ramalingam, Gabriele Bocelli, Murugesan Saravanan, Lara Righi, YuriiChumakov, Andrea Cantoni; Resources: Kuppukkannu Ramalingam, Gabriele Bocelli; Data Curation: Kuppukkannu Ramalingam, Murugesan Saravanan; Writing - Original Draft: Kuppukkannu Ramalingam; Writing - Review and Editing: Murugesan Saravanan; Visualization: Kuppukkannu Ramalingam, Murugesan Saravanan; Supervision: Kuppukkannu Ramalingam; Project Administration: Kuppukkannu Ramalingam.

ORCID and Email

Kuppukkannu Ramalingam
krauchem@yahoo.com
https://orcid.org/0000-0001-8689-8007
Murugesan Saravanan
sarchem@yahoo.com
https://orcid.org/0000-0003-4740-307X
Gabriele Bocelli
bocelli@unipr.it
https://orcid.org/0000-0003-3196-8885
Lara Righi
lara.righi@unipr.it
https://orcid.org/0000-0001-9372-5438
Yurii Chumakov
chumakov@phys.asm.md
https://orcid.org/0000-0003-2582-2871
Andrea Cantoni
provolo@pop.unipr.it
https://orcid.org/0000-0001-7224-3253

References

[1]. Angeloski, A.; Cortie, M. B.; Scott, J. A.; Bordin, D. M.; McDonagh, A. M. Conversion of single crystals of a nickel(II) dithiocarbamate complex to nickel sulfide crystals. *Inorganica Chim. Acta* **2019**, *487*, 228–233.

[2]. Yan, Y.; Krishnakumar, S.; Yu, H.; Ramishetti, S.; Deng, L.-W.; Wang, S.; Huang, L.; Huang, D. Nickel(II) dithiocarbamate complexes containing sulforhodamine B as fluorescent probes for selective detection of nitrogen dioxide. *J. Am. Chem. Soc.* **2013**, *135*, 5312–5315.

[3]. Roffey, A.; Hollingsworth, N.; Hogarth, G. Synthesis of ternary sulfide nanomaterials using dithiocarbamate complexes as single source precursors. *Nanoscale Adv.* **2019**, *1*, 3056–3066.

[4]. Al-Jibori, S. A.; Al-Janabi, A. S. M.; Al-Sahan, S. W. M.; Wagner, C. Pd (II)-pyrrolidine dithiocarbamate complexes: Synthesis, spectroscopic studies and molecular structure of [Pd(PyDT)(ppy)]. *J. Mol. Struct.* **2021**, *1227*, 129524.

[5]. Liu, Y.; Xing, Z.; Zhang, X.; Liang, G. Inorganic anion-dependent assembly of zero-, one-, two- and three-dimensional Cu(II)/Ag(I) complexes under the guidance of the HSAB theory: Synthesis, structure, and magnetic property. *J. Solid State Chem.* **2017**, *246*, 48–56.

[6]. Hogarth, G. Metal-dithiocarbamate complexes: chemistry and biological activity. *Mini Rev. Med. Chem.* **2012**, *12*, 1202–1215.

[7]. Ramalingam, K.; Srinivasan, S.; Rizzoli, C. Solvothermal preparation of nano cobalt sulfide from tris (cyclohexylpiperazinedithiocarbamato) cobalt(III) and characterization, single crystal X-ray crystal structure of the precursor. *J. Coord. Chem.* **2021**, *73*, 3487–3499.

[8]. Ramalingam, K.; Srinivasan, S. Synthesis, spectral, single crystal X-ray structural, CShM and BVS characterization of iron(III) cyclohexyl dithiocarbamates and their solvothermal decomposition to nano iron(II) sulphide. *J. Mol. Struct.* **2015**, *1100*, 290–298.

[9]. Manohar, A.; Ramalingam, K.; Thiruneelakandan, R.; Bocelli, G.; Righi, L. Steric and electronic effects of chelating phosphines: Synthesis, spectral, and single crystal X-ray structural studies on [1,3-bis(di phenylphosphino-k,P,P′)propane](diisopropyldithiocarbamato) nickel (II) perchlorate and [1,3-bis(diphenylphosphino-k,P,P′)propane](pi peridinecarbodithioato)nickel(II) perchlorate. *Z. Anorg. Allg. Chem.* **2001**, *627*, 1103–1108.

[10]. Arshad, M.; Wang, Z.; Nasir, J. A.; Amador, E.; Jin, M.; Li, H.; Chen, Z.; Rehman, Z. U.; Chen, W. Single source precursor synthesized CuS nanoparticles for NIR phototherapy of cancer and photodegradation of organic carcinogen. *J. Photochem. Photobiol. B* **2021**, *214*, 112084.

[11]. Roffey, A.; Hollingsworth, N.; Islam, H.-U.; Mercy, M.; Sankar, G.; Catlow, C. R. A.; Hogarth, G.; de Leeuw, N. H. Phase control during the synthesis of nickel sulfide nanoparticles from dithiocarbamate precursors. *Nanoscale* **2016**, *8*, 11067–11075.

[12]. Ramalingam, K.; Srinivasan, S.; Ethirajavalli, R.; Rizzoli, C. Quantification of distortions associated with planar NiS4, NiS2NP and NiS2P2 chromophores: Synthesis, structural and CSM analysis. *Polyhedron* **2016**, *104*, 138–144.

[13]. Srinivasan, S.; Ramalingam, K.; Rizzoli, C. Trans influence and steric effect on the distortions in planar NiS4, NiS2PN, and NiS2P2 chromophores. *Z. Anorg. Allg. Chem.* **2012**, *638*, 1356–1361.

[14]. Srinivasan, S.; Ramalingam, K.; Rizzoli, C. Synthesis, NMR and single crystal X-ray structural studies on planar NiS4 and NiS2PN chromophores: Steric and electronic effects. *Polyhedron* **2012**, *33*, 60–66.

[15]. Bhaskaran, R.; Ramalingam, K.; Bocelli, G.; Cantoni, A.; Rizzoli, C. Steric and electronic effects of N -coordinated NC − and NCS− on NiS2PN: synthesis, spectral and single crystal X-ray structural studies on N, N ′-di- n -butyldithiocarbamate complexes of nickel(II) with phosphorus and nitrogen donor ligands. *J. Coord. Chem.* **2008**, *61*, 1710–1719.

[16]. Arul Prakasam, B.; Ramalingam, K.; Bocelli, G.; Cantoni, A. Steric and electronic effects of substituents on planar nickel(II) complexes: Synthesis, NMR spectral and single crystal X-ray structural studies on nickel(II) dithiocarbamates with NiS2PN, NiS2PC, and NiS2P2 Chromophores. *Bull. Chem. Soc. Jpn.* **2006**, *79*, 113–117.

[17]. Thiruneelakandan, R.; Ramalingam, K.; Bocelli, G.; Righi, L. Synthesis, spectral, cyclic voltammetric studies, and single crystal X-ray structure determination of the planar NiS2P2, NiS2PN, and NiS2PC chromophores. *Z. Anorg. Allg. Chem.* **2005**, *631*, 187–193.

[18]. Ramalingam, K.; Thiruneelakandan, R.; Bocelli, G.; Righi, L. Trans influence of triphenylphosphines and pseudohalogens on Ni-S bonds: Synthesis, spectral and single crystal X-ray structural studies on NiS2PN and NiS2PC chromophores. *Open Chem.* **2012**, *10*, 1199–1207.

[19]. Bobinihi, F. F.; Onwudiwe, D. C.; Ekennia, A. C.; Okpareke, O. C.; Arderne, C.; Lane, J. R. Group 10 metal complexes of dithiocarbamates derived from primary anilines: Synthesis, characterization, computational and antimicrobial studies. *Polyhedron* **2019**, *158*, 296–310.

[20]. Han, J.; Zhang, W.; Zhou, T.; Wang, X.; Xu, R. Nickel-complexes with a mixed-donor ligand for photocatalytic hydrogen evolution from aqueous solutions under visible light. *RSC Adv.* **2012**, *2*, 8293–8296.

[21]. Gao, M.-R.; Xu, Y.-F.; Jiang, J.; Yu, S.-H. Nanostructured metal chalcogenides: synthesis, modification, and applications in energy conversion and storage devices. *Chem. Soc. Rev.* **2013**, *42*, 2986–3017.

[22]. Kershaw, S. V.; Susha, A. S.; Rogach, A. L. Narrow bandgap colloidal metal chalcogenide quantum dots: synthetic methods, heterostructures, assemblies, electronic and infrared optical properties. *Chem. Soc. Rev.* **2013**, *42*, 3033–3087.

[23]. Abu-Surrah, A. S.; Kettunen, M. Platinum group antitumor chemistry: design and development of new anticancer drugs complementary to cisplatin. *Curr. Med. Chem.* **2006**, *13*, 1337–1357.

[24]. Weiss, R. B.; Christian, M. C. New cisplatin analogues in development. A review: A Review. *Drugs* **1993**, *46*, 360–377.

[25]. Lebwohl, D.; Canetta, R. Clinical development of platinum complexes in cancer therapy: an historical perspective and an update. *Eur. J. Cancer* **1998**, *34*, 1522–1534.

[26]. Wong, E.; Giandomenico, C. M. Current status of platinum-based antitumor drugs. *Chem. Rev.* **1999**, *99*, 2451–2466.

[27]. Amable, L. Cisplatin resistance and opportunities for precision medicine. *Pharmacol. Res.* **2016**, *106*, 27–36.

[28]. Reedijk, J. Improved understanding in platiniumantitumour chemistry. *Chem. Commun. (Camb.)* **1996**, *7*, 801–806.

[29]. Miller, R. P.; Tadagavadi, R. K.; Ramesh, G.; Reeves, W. B. Mechanisms of cisplatin nephrotoxicity. *Toxins (Basel)* **2010**, *2*, 2490–2518.

[30]. Milbeo, P.; Quintin, F.; Moulat, L.; Didierjean, C.; Martinez, J.; Bantreil, X.; Calmès, M.; Lamaty, F. Synthesis, characterisation and cytotoxic activity evaluation of new metal-salen complexes based on the 1,2-bicyclo[2.2.2]octane bridge. *Tetrahedron Lett.* **2021**, *63*, 152706.

[31]. Bruker (2009). SADABS. Bruker AXS Inc., Madison, Wisconsin, USA.

[32]. Bruker AXS, Inc.6300, Enterprise Lane, Madison, Wi. 5179-1173. USA.

[33]. Dolomanov, O. V.; Bourhis, L. J.; Gildea, R. J.; Howard, J. A. K.; Puschmann, H. OLEX2: a complete structure solution, refinement and analysis program. *J. Appl. Crystallogr.* **2009**, *42*, 339–341.

[34]. Faruggia, L. J. ORTEP-3 for Windows, University of Glassgow, Scotland, U K, 1999.

[35]. Macrae, C. F.; Sovago, I.; Cottrell, S. J.; Galek, P. T. A.; McCabe, P.; Pidcock, E.; Platings, M.; Shields, G. P.; Stevens, J. S.; Towler, M.; Wood, P. A. Mercury 4.0: from visualization to analysis, design and prediction. *J. Appl. Crystallogr.* **2020**, *53*, 226–235.

[36]. Sharma, M.; Kumar, L.; Jain, A.; Verma, V.; Sharma, V.; Kushwaha, B.; Lal, N.; Kumar, L.; Rawat, T.; Dwivedi, A. K.; Maikhuri, J. P.; Sharma, V. L.; Gupta, G. Designed chemical intervention with thiols for prophylactic contraception. *PLoS One* **2013**, *8*, e67365.

[37]. Engelhardt, L. M.; Patrick, J. M.; White, A. H. Crystal Structures of Bis(pyrrolidinedithiocarbamato)-nickel(II) and -copper(II) (Redeterminations). *Aust. J. Chem.* **1985**, *38*, 1413–1416.

[38]. Batsanov, A. S.; Howard, J. A. K. trans-Dichlorobis(triphenyl phosphine)nickel(II) bis(dichloromethane) solvate: redetermination at 120 K. *Acta Crystallogr. Sect. E Struct. Rep. Online* **2001**, *57*, m308–m309.

[39]. Brammer, L.; Stevens, E. D. Structure of dichlorobis(triphenyl phosphine)nickel(II). *Acta Crystallogr. C* **1989**, *45*, 400–403.

[40]. Cao, R.; Li, X.; Sun, H. Synthesis and properties of nickel(II) complexes containing trimethylphosphine and thiophenolato-ligands. *Z. Anorg. Allg. Chem.* **2007**, *633*, 2305–2309.

[41]. Ramalingam, K.; Aravamudan, G.; Seshasayee, M.; Verghese, B. Structure of bis(monothiobenzoato-S)[ethylenebis(diphenylphos phino)] nickel(II). *Acta Crystallogr. C* **1987**, *43*, 471–473.

[42]. Milburn, G. H. W.; Truter, M. R. The crystal structures of cis- and trans-dichlorodiammineplatinum(II). *J. Chem. Soc.* **1966**, 1609–1616.

[43]. Brown, I. D. The bond valence model as a tool for teaching inorganic chemistry: The ionic model revisited. *J. Chem. Educ.* **2000**, *77*, 1070.

[44]. Brese, N. E.; O'Keeffe, M. Bond-valence parameters for solids. *Acta Crystallogr. B* **1991**, *47*, 192–197.

[45]. O'Keefe, M.; Brese, N. E. Atom sizes and bond lengths in molecules and crystals. *J. Am. Chem. Soc.* **1991**, *113*, 3226–3229.

[46]. Liu, W.; Thorp, H. H. Bond valence sum analysis of metal-ligand bond lengths in metalloenzymes and model complexes. 2. Refined distances and other enzymes. *Inorg. Chem.* **1993**, *32*, 4102–4105.

[47]. Ok, K. M.; Halasyamani, P. S.; Casanova, D.; Llunell, M.; Alemany, P.; Alvarez, S. Distortions in octahedrally coordinated d0 transition metal oxides: A continuous symmetry measures approach. *Chem. Mater.* **2006**, *18*, 3176–3183.

[48]. Alvarez, S.; Avnir, D.; Llunell, M.; Pinsky, M. Continuous symmetry maps and shape classification. The case of six-coordinated metal compounds Electronic supplementary information (ESI) available: tables of CSD refcodes, structural parameters and symmetry measures for the studied compounds. See http://www.rsc.org/suppdata/nj/b2/b202096n/. *New J. Chem.* **2002**, *26*, 996–1009.

[49]. Zabrodsky, H.; Peleg, S.; Avnir, D. Continuous symmetry measures. *J. Am. Chem. Soc.* **1992**, *114*, 7843–7851.